

<https://doi.org/10.1038/s41699-024-00467-8>

Hometronics – accessible production of graphene suspensions for health sensing applications using only household items

Check for updates

Adel K. A. Aljarid^{1,4}, Jasper Winder^{1,4}, Cencen Wei^{1,4}, Arvind Venkatraman², Oliver Tomes³, Aaron Soul³, Dimitrios G. Papageorgiou³, Matthias E. Möbius² & Conor S. Boland¹ ✉

Nanoscience at times can seem out of reach to the developing world and the general public, with much of the equipment expensive and knowledge seemingly esoteric to nonexperts. Using only cheap, everyday household items, accessible research with real applications can be shown. Here, graphene suspensions were produced using pencil lead, tap water, kitchen appliances, soaps and coffee filters, with a children's glue-based graphene nanocomposite for highly sensitive pulse measurements demonstrated.

Research into using liquid exfoliation (LE) methods have led to the widespread production of two-dimensional (2D) materials on a large scale¹. Particularly, the demonstration of shear exfoliation methods² has made LE more viable for low-cost production via the use of household food processors^{3,4}. However, low-income institutions, third world countries and citizen science initiatives would still struggle. As beyond the shearing device, the purifying instruments (i.e., centrifuge), exfoliation medium (i.e. solvents or deionised water) and industrial graphite sources that are commonly applied in research⁵ are still economically exclusive⁶. Here, we demonstrate that a pencil can be processed into a powder and LE in a blender to isolate a suspension of high-quality graphene in tap water using a coffee filter (Fig. 1a). Furthermore, we show that by using school glue, a nanocomposite we call pencil putty (p-putty) can be produced for impactful health applications. The total overall costing of this project was a mere £76.22 (equivalent to ~\$96.67, Supplementary Table 1), greatly facilitating its accessibility.

In Fig. 1b–e, we show the pencil and blender (with graphene suspension contained inside before and after blending) utilised in the study, as well as the stable graphene suspension produced. Exfoliation of the pencil lead occurs via the blender's blades generating turbulent shear rates $>10^4 \text{ s}^{-1}$, resulting in shear-induced interlayer sliding and the delamination of graphene nanosheets from bulk graphite crystals². For the exfoliation medium, a mixture of dish soap in tap water was used. Here, the dish soap acts as an electrostatic stabilising agent for the exfoliated nanosheets to both suspend the non-polar graphene in the polar water medium and to prevent against graphene aggregation⁷. This mitigation occurs through the amphiphilic soap absorbing onto individual

nanosheets, with the non-polar tail group of the soap on the basal plane and the polar head group extending and mixing with the water⁷. In the past, shear exfoliation utilising household soaps resulted in a thick foam layer that made large amounts of graphite inaccessible to shearing^{2,3}. To overcome these issues, fabric softener was also added to the blend to suppress foaming. After several exfoliation intervals (see Methods), the resultant suspension was passed through a coffee filter with a pore diameter of $\sim 10 \mu\text{m}$. This resulted in the collection of large particulates of unexfoliated graphite on the coffee filter, with the suspension that passed through gathered in a flask. Using atomic force microscopy (AFM) on the filtered suspension, the pencil lead was confirmed to have been exfoliated into nanosheets in Fig. 1d. We also note the suspensions created were polydisperse, indicative of single step size selection procedures⁸, with the presence of larger ($> 700 \text{ nm}$) and small ($< 100 \text{ nm}$) nanosheets observed. Through Raman spectroscopy in Fig. 1e, the production of graphene was confirmed through a comparative analysis of the powdered and exfoliated pencil lead spectra. All characteristic modes associated with graphitic material were present in both samples at Raman shifts of $\sim 1350 \text{ cm}^{-1}$, $\sim 1580 \text{ cm}^{-1}$, and $\sim 2700 \text{ cm}^{-1}$, which relate to the D, G and 2D modes respectively⁹. Specifically looking at the 2D modes of the samples, there is a downshift from the powdered ($\sim 2705 \text{ cm}^{-1}$) to the exfoliated ($\sim 2697 \text{ cm}^{-1}$) material, indicative of LE leading to multi-layered graphene¹⁰. We also observed the D mode intensity to increase upon exfoliation, due to decreased nanosheet areal size and increased defect density associated with edge sites¹¹. This is an intrinsic feature of the LE method, with nanosheet area and thickness coupled to one another (i.e. thin nanosheets will always have a small areal size)¹². Using standardised spectroscopic metrics¹¹, information with regards to the graphene's mean

¹School of Mathematical and Physical Sciences, University of Sussex, Brighton BN1 9QH, UK. ²School of Physics, AMBER and CRANN Research Centres, Trinity College Dublin, Dublin 2, Ireland. ³School of Engineering and Materials Science, Queen Mary University, London E1 4NS, UK. ⁴These authors contributed equally: Adel K. A. Aljarid, Jasper Winder, Cencen Wei. ✉ e-mail: c.s.boland@sussex.ac.uk

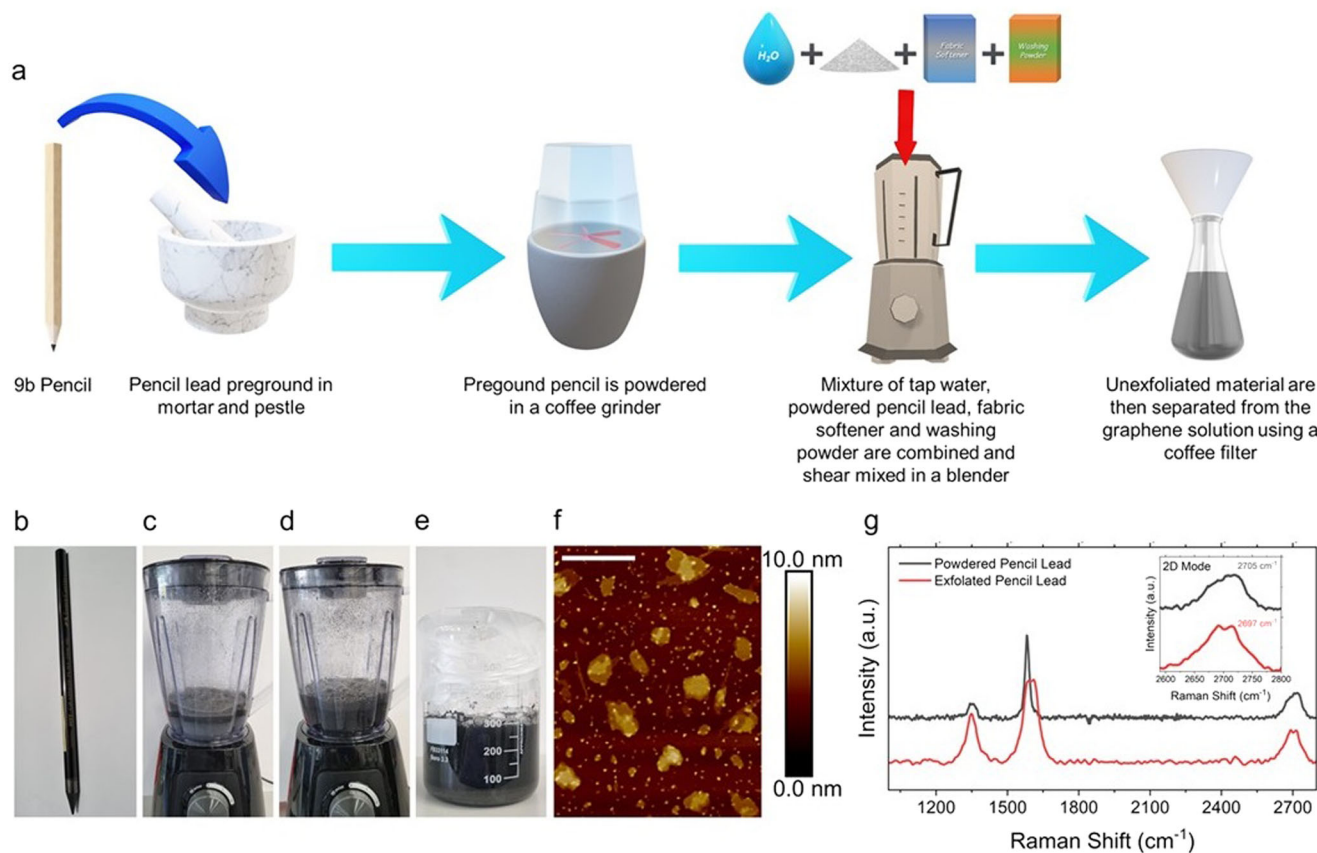


Fig. 1 | Graphene production from household commercial items. **a** Scheme presenting graphene LPE using a pencil. **b–e** Photographs of the 9b pencil (**b**), commercial blender before (**c**) and after (**d**) blending and a graphene suspension after

sitting for 24 h (**e**). **f** Representative AFM micrograph of pencil-based graphene nanosheets. Scale bar is 1000 nm. **g** Raman spectroscopy of powdered and exfoliated pencil lead. Inset, closer look at 2D modes of the respective spectra.

length ($\langle L \rangle$) in μm ,

$$\langle L \rangle = \frac{0.094}{(I_D/I_G)_{\text{Graphene}} - (I_D/I_G)_{\text{Graphite}}} \quad (1)$$

And mean layer number ($\langle N \rangle$),

$$\langle N \rangle = 1.04 \cdot \left[(I_{2D}/I_G)_{\text{Graphene}} \right]^{-2.32} \quad (2)$$

can be derived from the Raman spectra. Where $(I_D/I_G)_{\text{Graphene}}$ and $(I_D/I_G)_{\text{Graphite}}$, are the ratios between the D and G mode intensities for graphene and the starting graphite source respectively. Furthermore, $(I_{2D}/I_G)_{\text{Graphene}}$ is the ratio between the 2D and G mode intensities. Using Eqs. 1 and 2, for our home-made graphene, $\langle L \rangle \sim 314 \pm 63 \text{ nm}$ and $\langle N \rangle \sim 7.37 \pm 1.84$ respectively. In comparison to standard lab processed graphene, similar aspect ratio values were reported¹³.

In addition to demonstrating purely kitchen appliance-based graphene production, we also show that the resultant nanosheets can be applied in an equally accessible application with powerful research outcomes. Using a commercial water-based polyvinyl alcohol (PVA) children’s glue kit, graphene could be added via solution mixing to create p-putty (Fig. 2a). This nanocomposite was based on a boron crosslinked hydrogel created from mixing Elmer’s PVA glue with a boric acid solution known as Elmer’s Magic Liquid. We found that the addition of the graphene to pristine putty darkened the hue of the material, with the presence of graphene also turning the putty from an insulator to an electrical conductor (Supplementary Figure 1). Through scanning electron microscopy (SEM), the topography between the pristine (Fig. 2b) and a graphene loaded sample (Fig. 2c) are also seen to greatly differ. Mechanically, the addition of graphene to the putty had no

effect on either the Young’s modulus (Y) in Fig. 2d nor the other mechanical properties (Supplementary Figures 2 and 3) of the nanocomposites as a function of volume fraction (V_f). This invariance in mechanical properties is a common occurrence when pristine graphene was mixed into a hydrogel matrix due to its hydrophobic nature^{13,14}. This invariance is likely due to poor interfacial interactions between the hydrophobic graphene filler and hydrophilic PVA matrix, resulting in weak stress transfer from matrix to filler¹⁵. In the case of p-putty, it resulted in a material that remained very pliable (Supplementary movie). However, it was noted that at higher loadings ($V_f \sim 0.6\%$), visible graphene aggregation occurred in the samples, which resulted in mechanical properties to marginally increase. Through rheological measurements in Fig. 2e, a 0.4% p-putty sample behaved similarly to the unloaded equivalent as a function of shear strain. Both materials presented Maxwell fluid behaviour, with a relaxation time of $\sim 2 \text{ s}$ and a viscosity $\sim 3000 \text{ Pa}\cdot\text{s}$ (Supplementary Figure 4).

Previously, the addition of sonic probe exfoliated graphene to a boric acid cross-linked polysilicone, commercially known as silly putty, resulted in a soft viscoelastic nanocomposite with record high electromechanical properties¹⁶. The advantage of p-putty over its silly putty variant is the user-friendly nature of its production. With graphene silly putty requiring the use of N-Methyl-2-pyrrolidone and chloroform, two expensive and highly toxic solvents. Similar to graphene silly putty, upon the application of compressive strain ($-\epsilon$), the electrical properties of p-putty were also observed to rapidly change. In Fig. 2f, fractional resistance change ($\Delta R/R_0$) as a function of $-\epsilon$ for a select range of V_f increased linearly in accordance with electromechanical theory¹⁷. Using the following expression

$$G = \frac{\Delta R}{R_0} \cdot \epsilon^{-1} \quad (3)$$

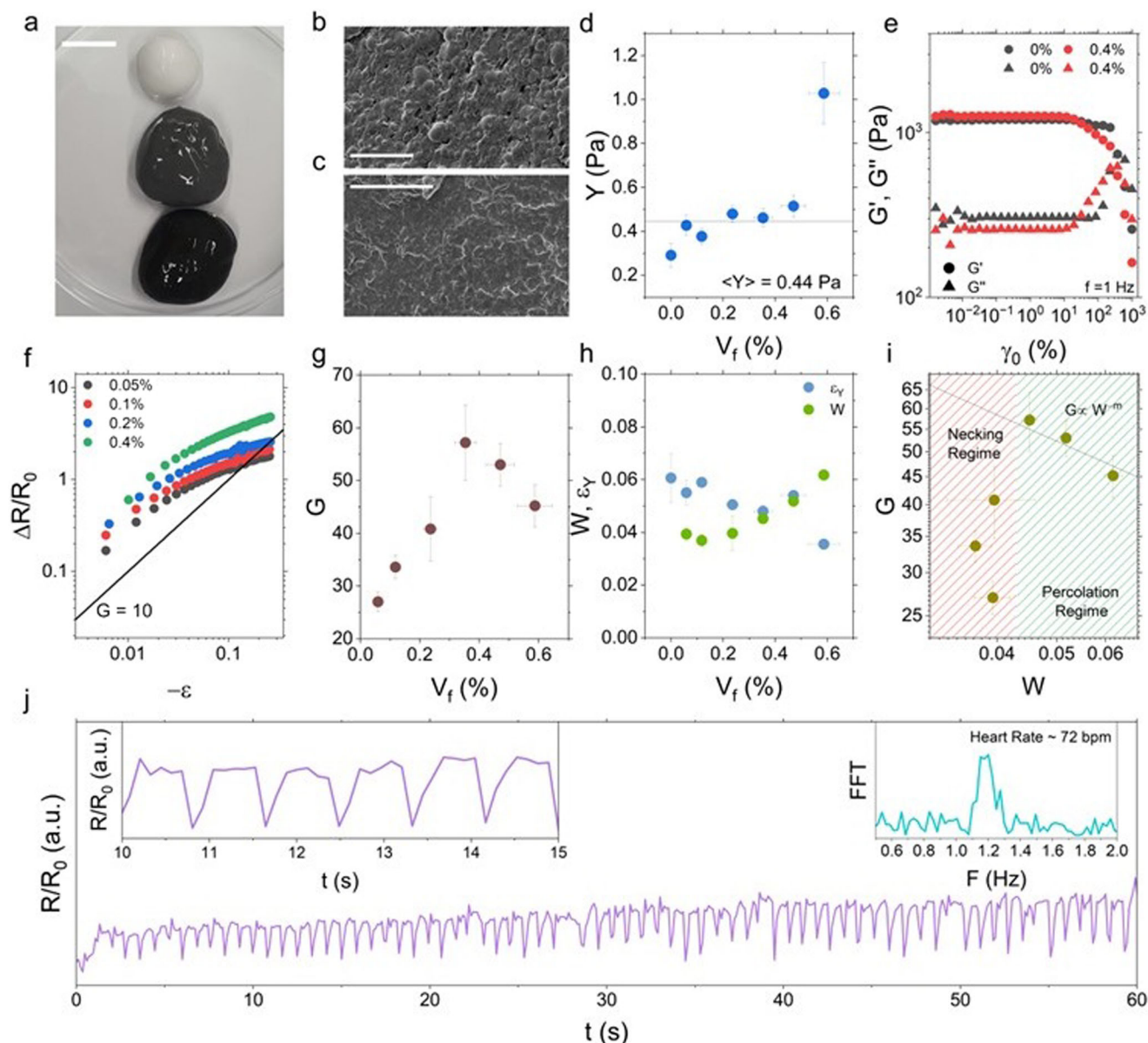


Fig. 2 | P-putty nanocomposite. **a** Photograph of p-putty with 0%, 0.1%, and 0.4% graphene volume fraction (V_f), top to bottom. Scale bar is 2 cm. **b, c** SEM micrographs of pristine putty (**b**) and 0.4% p-putty (**c**). Scale bars are 10 μm and 25 μm respectively. **d** Compressive Young's Modulus (Y) as a function of V_f . Solid line represents mean value. **e** Shear storage (G') and loss (G'') moduli of pristine and 0.4% putty versus shear strain amplitude (γ_0). **f** Fractional resistance change ($\Delta R/R_0$) as a function of compression strain for a select range of V_f . Solid line is a fit of Eq. 3, where

gauge factor (G) = 10. **g** P-putty gauge factor (G) as a function of V_f . **h** P-putty working factor (W) and yield strain versus V_f . **i** P-putty gauge (G) and working (W) factors plotted against one another scaled with a power-law exponent associated with the Kraus constant (m) in the percolation regime. **j** Pulse as a function of time. Insets, zoomed in view of pulse signal (lefthand side) and fast Fourier transform (FFT) of pulse data showing a rate of ~ 1.2 Hz (righthand side).

The electromechanical sensitivity (G) can be extrapolated by fitting Eq. 3 to the low strain regimes of $\Delta R/R_0$ versus $-\epsilon$ curves (Supplementary Figure 5), with G values plotted as a function of V_f in Fig. 2g. As standard, G generally is a maximum near the percolation threshold due to minimised network connections and decreases with V_f as connections increase¹⁸. We however note that due to common network necking effects^{14,19}, which leads to inefficient strain transfer to the network during deformation, G increased from ~ 27 at $\sim 0.1\%$ to ~ 57 at $\sim 0.4\%$ and subsequently decreased to ~ 45 at $\sim 0.6\%$. In comparison to other hydrogel¹⁴ and mixed-phase¹⁷ nanocomposite strain sensors, G is generally < 50 ²⁰. Through Supplementary Figure 5, another important performance metric which dictates the value of G , can also be derived from the strain limit of the linear regime. This metric, the working factor (W), is simply extrapolated from the fit of Eq. 3 and is the absolute strain value at which

the data deviates from the fitting. Plotting W versus V_f in Fig. 2h, alongside the yield strain (ϵ_Y). As expected¹⁷, values for W and ϵ_Y were found to overlay one another due to their intrinsic connection. In Fig. 2i, G as a function of W showed that in the necking regime W was invariant¹⁴. However, in the percolation regime, W scaled with an exponent of $-m$ ^{13,20}. Where m is the Kraus constant and has a value of 0.5. With p-putty's combination of exceedingly soft stiffness and large electromechanical sensitivity, the nanocomposite was capable of measuring heart rate as a function of time (Fig. 2j). When a p-putty based electronic patch (see Methods) was held to the carotid artery in the neck, we report a steady state signal and through fast Fourier transform (FFT) analysis a healthy pulse frequency of ~ 1.2 Hz (equivalent to 72 bpm).

In this communication, we introduce hometeronics as not only a valid way in which nanoscience can be accessible to all researchers and the public

alike, but a simple methodology with real applications from our everyday surroundings. Nanoscience research need not be complex and by taking pencil lead processed using home appliances, we demonstrate graphene suspensions from household detergents. Using home-based graphene, nanocomposites from children's glue can be produced to easily measure a wearer's pulse. The accessibility of the work also leads to the use of the methodologies being applied in schools with students from a range of economic backgrounds to inspire and diversify the next generation of scientists.

Methods

Graphene exfoliation

A Graphite Pure 2900 9B pencil was initially crushed in a mortar and pestle, then ground in a SQ Professional Blitz Coffee Grinder - Spice Grinding Mill - One-Touch for ~60 s. A mass of 2.5 g of Fairy Max Power Washing Up Liquid was then mixed with 1 L of tap water. 300 mL of the soap mixture was then added to a Tefal BL420840 Blendforce II Blender (Plastic Jug, 600 W, 1.5 L) with 1 mL of Ecover Fabric Softener also added to the blender. 16 g of powdered pencil lead was then placed in the blender and stirred into the soap/softener/water mixture by hand. The blender was then turned on to the first (#1) setting for 1-minute on, 1 minute off intervals to reduce motor heating effects, until the total blending time reached 15 minutes. The solution was then transferred to a beaker and left to sit for 24 h. After which, the solution was passed through a Rombouts Italian No. 2 Coffee Filter.

Atomic force microscopy

Diluted graphene suspension (~0.01 mg/mL) was drop cast onto a heated silicon wafer (70 °C). The wafer was then washed with deionized water to remove residual household soaps. A Dimension Icon Bruker in an insulated box over an anti-vibrant stage to minimise environmental noise and building vibrations was used for measurement. A ScanAsyst Air tip with a spring constant of 0.4 N m⁻¹ and a tip-sample contact force of 5.0 nN was used.

Raman spectroscopy

Graphene suspension (6 mg/mL) was drop cast onto a heated silicon wafer (70 °C). The wafer was then washed with deionized water to remove residual household soaps. For the graphite sample, pencil lead was crushed using the mortar and pestle and patted down onto a silicon wafer. Renishaw inVia confocal Raman microscope with 0.8 cm⁻¹ spectral resolution and a 532 nm laser (type: solid state, model: RL53250) was used for measurements. A 2400 mm⁻¹ grating at 100× magnification and 5 mW laser power was applied. Each sample curve is an average of ten spectra.

P-putty production

For the graphene sample preparation, 2 mL of Elmer's White PVA Glue, 1 mL of Elmer's Glue Slime Magical Liquid Solution, and 0.5 mL of graphene suspension were mixed by hand for approximately 5 to 7 minutes. To vary the graphene loading, different concentration suspensions, ranging from 1 mg/mL to 10 mg/mL, were used. For the pristine putty sample, in place of the graphene suspension, 0.5 mL of tap water was used. For all p-putty samples, they were left at room temperature for 40 minutes before testing.

Scanning electron microscopy

The fracture surfaces of the nanocomposites were observed using scanning electron microscopy (SEM, FEI Inspect-F, The Netherlands) with an acceleration voltage of 5 kV. The nanocomposites were cryo-fractured after immersion in liquid N₂ and carbon coated with a ≈ 5 nm layer.

Electro-mechanical measurements

A Stable Micro Systems TA-TXplus texture analyser with two insulating plates was used. Electrically conductive copper tape was attached to the inside of their faces. The copper tape contacts were

then attached to a Keithley 2614B source metre using silver wire to supply a current across the samples. P-putty samples cyclical in shape (diameter = 5.5 mm and length 6 mm) were placed onto the bottom stationary plate's copper tape contact, with the test arm lowering the second plate's copper tape contact into contact with the top of the sample. Through this setup, mechanical (texture analyser) and electrical (source metre) data could be simultaneously recorded. Samples were deformed at a rate of 6 mm/min through the application of compressive strain (i.e. the second plate lowering) for all mechanical and electromechanical measurements.

Rheology

For measurements, an Anton Paar MCR 302e rheometer was used. Samples were flattened prior to lowering the plates (25 mm diameter). Gap size was 1.1 mm, with normal force quickly settling to zero after reaching gap height. Samples were subsequently allowed to relax for 30 minutes while oscillating the plate at low amplitude (0.1% strain amplitude at 1 Hz).

Pulse measurements

An electronic patch made out of Ecoflex 00–30 using a previously described method was used to encapsulate the putty sample for testing¹³. Using this methodology, a thin (~1 mm), 1 cm² p-putty sample with a ~0.4 vol% graphene loading was used. For pulse testing it was performed by Adel K.A. Aljarid on his own person by holding the electronic patch to the carotid artery in the neck.

Data availability

The authors declare that all data supporting the findings are available within the communication and/or its supplementary information.

Received: 18 January 2024; Accepted: 22 March 2024;

Published online: 30 March 2024

References

1. Pinilla, S., Coelho, J., Li, K., Liu, J. & Nicolosi, V. Two-dimensional material inks. *Nat. Rev. Mater.* **7**, 717–735 (2022).
2. Paton, K. R. et al. Scalable production of large quantities of defect-free few-layer graphene by shear exfoliation in liquids. *Nat. Mater.* **13**, 624–630 (2014).
3. Varla, E. et al. Turbulence-assisted shear exfoliation of graphene using household detergent and a kitchen blender. *Nanoscale* **6**, 11810–11819 (2014).
4. Pérez-Álvarez, D. T., Brown, J. & Stafford, J. Modification of kitchen blenders into controllable laboratory mixers for mechanochemical synthesis of atomically thin materials. *HardwareX* **16**, e00471 (2023).
5. Backes, C. et al. Guidelines for exfoliation, characterization and processing of layered materials produced by liquid exfoliation. *Chem. Mater.* **29**, 243–255 (2017).
6. Ravindran, S. How DIY technologies are democratizing science. *Nature* **587**, 509–511 (2020).
7. Griffin, A. et al. Effect of surfactant choice and concentration on the dimensions and yield of liquid-phase-exfoliated nanosheets. *Chem. Mater.* **32**, 2852–2862 (2020).
8. Backes, C. et al. Production of highly monolayer enriched dispersions of liquid-exfoliated nanosheets by liquid cascade centrifugation. *ACS Nano* **10**, 1589–1601 (2016).
9. Ferrari, A. C. et al. Raman spectrum of graphene and graphene layers. *Phys. Rev. Lett.* **97**, 187401 (2006).
10. Ferrari, A. C. & Basko, D. M. Raman spectroscopy as a versatile tool for studying the properties of graphene. *Nat. Nanotechnol.* **8**, 235–246 (2013).
11. Backes, C. et al. Spectroscopic metrics allow in situ measurement of mean size and thickness of liquid-exfoliated few-layer graphene nanosheets. *Nanoscale* **8**, 4311–4323 (2016).

12. Backes, C. et al. Equipartition of energy defines the size–thickness relationship in liquid-exfoliated nanosheets. *ACS Nano* **13**, 7050–7061 (2019).
 13. Aljarid, A. K. A. et al. Smart skins based on assembled piezoresistive networks of sustainable graphene microcapsules for high precision health diagnostics. *Adv. Funct. Mater.* **33**, 2303837 (2023).
 14. Aljarid, A. A. K., Doty, K. L., Wei, C., Salvage, J. P. & Boland, C. S. Food-inspired, high-sensitivity piezoresistive graphene hydrogels. *ACS Sustain Chem. Eng.* **11**, 1820–1827 (2023).
 15. Wang, W., Li, Z., Marsden, A. J., Bissett, M. A. & Young, R. J. Mechanisms of reinforcement of PVA-based nanocomposites by hBN nanosheets. *Compos. Sci. Technol.* **218**, 109131 (2022).
 16. Boland, C. S. et al. Sensitive electromechanical sensors using viscoelastic graphene-polymer nanocomposites. *Science* **354**, 1257–1260 (2016).
 17. Boland, C. S. Stumbling through the research wilderness, standard methods to shine light on electrically conductive nanocomposites for future healthcare monitoring. *ACS Nano* **13**, 13627–13636 (2019).
 18. Boland, C. S. Approaching the limit of electromechanical performance in mixed-phase nanocomposites. *ACS Appl. Nano Mater.* **3**, 11240–11246 (2020).
 19. Boland, C. S., Khan, U., Benameur, H. & Coleman, J. N. Surface coatings of silver nanowires lead to effective, high conductivity, high-strain, ultrathin sensors. *Nanoscale* **9**, 18507–18515 (2017).
 20. Boland, C. S. Performance analysis of solution-processed nanosheet strain sensors – a systematic review of graphene and MXene wearable devices. *Nanotechnology* **35**, 202001 (2024).
- graphene suspensions. A.K.A.A. made the composite materials and performed electromechanical tests. O.T. performed SEM. A.V. performed rheological testing. C.S.B. analysed and modelled data. D.G.P., M.E.M., C.S.B. contributed materials, tools, and supervision. C.S.B wrote and revised the paper. A.K.A.A., C.W. and J.W. contributed equally to the work and may present themselves as the first author on their respective curriculum vitae.

Competing interests

The authors declare no competing interests.

Additional information

Supplementary information The online version contains supplementary material available at <https://doi.org/10.1038/s41699-024-00467-8>.

Correspondence and requests for materials should be addressed to Conor S. Boland.

Reprints and permissions information is available at <http://www.nature.com/reprints>

Publisher's note Springer Nature remains neutral with regard to jurisdictional claims in published maps and institutional affiliations.

Open Access This article is licensed under a Creative Commons Attribution 4.0 International License, which permits use, sharing, adaptation, distribution and reproduction in any medium or format, as long as you give appropriate credit to the original author(s) and the source, provide a link to the Creative Commons licence, and indicate if changes were made. The images or other third party material in this article are included in the article's Creative Commons licence, unless indicated otherwise in a credit line to the material. If material is not included in the article's Creative Commons licence and your intended use is not permitted by statutory regulation or exceeds the permitted use, you will need to obtain permission directly from the copyright holder. To view a copy of this licence, visit <http://creativecommons.org/licenses/by/4.0/>.

© The Author(s) 2024

Acknowledgements

C.W. and C.S.B. acknowledge funding from University of Sussex Strategic Development Fund. A.K.A.A. acknowledges funding through the Saudi Arabian Cultural Bureau. J.W. and C.S.B. acknowledge funding via the University of Sussex's 2023 Junior Research Associate Award Scheme. A.V. and M.E.M. acknowledge funding from Science Foundation Ireland grant SFI 17/CDA/4704.

Author contributions

C.S.B. conceived and designed experiments. J.W. created all graphene suspensions for the study. C.W. performed AFM and Raman on the